NASA TECHNICAL MEMORANDUM

NASA TM X-53535

1966

NASA TM X-53535

GPO PRICE $ _____

CFSTI PRICE(S) $ _____

Hard copy (HC) 3.00

Microfiche (MF) .65

ff 653 July 65

RESEARCH ACHIEVEMENTS REVIEW SERIES NO. 18

RESEARCH AND DEVELOPMENT OPERATIONS
GEORGE C. MARSHALL SPACE FLIGHT CENTER
HUNTSVILLE, ALABAMA

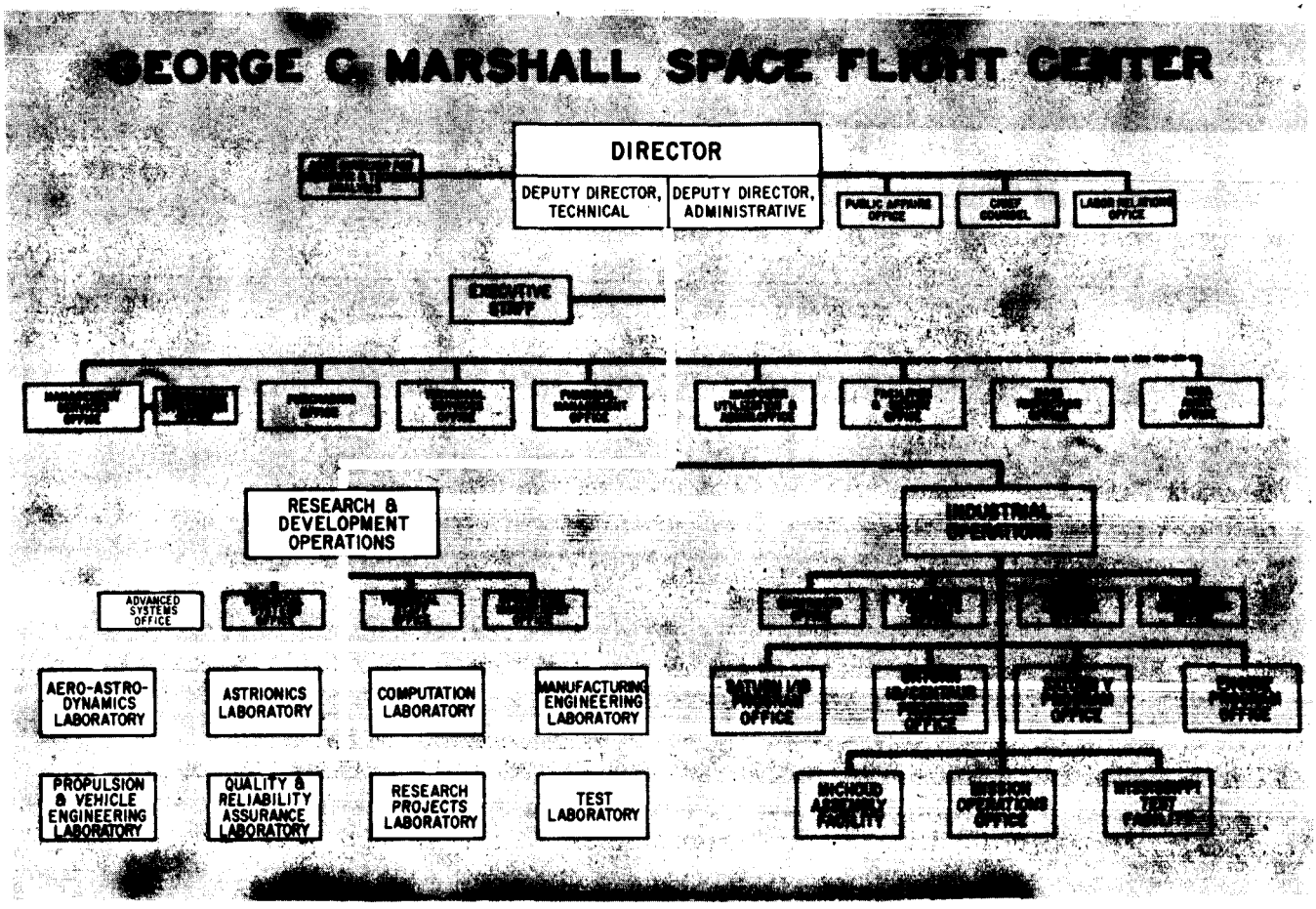

RESEARCH ACHIEVEMENTS REVIEW SERIES INCLUDES THE FOLLOWING FIELDS OF RESEARCH

1. RADIATION PHYSICS
2. THERMOPHYSICS
3. CHEMICAL PROPULSION
4. CRYOGENIC TECHNOLOGY
5. ELECTRONICS
6. CONTROL SYSTEMS
7. MATERIALS
8. MANUFACTURING
9. GROUND TESTING
10. QUALITY ASSURANCE AND CHECKOUT
11. TERRESTRIAL AND SPACE ENVIRONMENT
12. AERODYNAMICS
13. INSTRUMENTATION
14. POWER SYSTEMS
15. GUIDANCE CONCEPTS
16. ASTRODYNAMICS
17. ADVANCED TRACKING SYSTEMS
18. COMMUNICATION SYSTEMS
19. STRUCTURES
20. MATHEMATICS AND COMPUTATION
21. ADVANCED PROPULSION
22. LUNAR AND METEOROID PHYSICS

NASA TM X-53535

NATIONAL AERONAUTICS AND SPACE ADMINISTRATION
WASHINGTON, D. C.

COMMUNICATION SYSTEMS RESEARCH AT MSFC

RESEARCH ACHIEVEMENTS REVIEW SERIES NO. 18

RESEARCH AND DEVELOPMENT OPERATIONS
GEORGE C. MARSHALL SPACE FLIGHT CENTER
HUNTSVILLE, ALABAMA

1966

PREFACE

In 1955, the team which has become the Marshall Space Flight Center (MSFC) began to organize a research program within its various laboratories and offices. The purpose of the program was two-fold: first, to support existing development projects by research studies and second, to prepare future development projects by advancing the state of the art of rockets and space flight. Funding for this program came from the Army, Air Force, and Advanced Research Projects Agency. The effort during the first year was modest and involved relatively few tasks. The communication of results was, therefore, comparatively easy.

Today, more than ten years later, the two-fold purpose of MSFC's research program remains unchanged, although funding now comes from NASA Program Offices. The present yearly effort represents major amounts of money and hundreds of tasks. The greater portion of the money goes to industry and universities for research contracts. However, a substantial research effort is conducted in house at the Marshall Center by all of the laboratories. The communication of the results from this impressive research program has become a serious problem by virtue of its very voluminous technical and scientific content.

The Research Projects Laboratory, which is the group responsible for management of the consolidated research program for the Center, initiated a plan to give better visibility to the achievements of research at Marshall in a form that would be more readily usable by specialists, by systems engineers, and by NASA Program Offices for management purposes.

This plan has taken the form of frequent Research Achievements Reviews, with each review covering one or two fields of research. These verbal reviews are documented in the Research Achievements Review Series.

Ernst Stuhlinger
Director, Research Projects Laboratory

These papers presented January 27, 1966

TABLE OF CONTENTS

HYDROGEN MASER RESEARCH ACHIEVEMENTS AT MSFC

by John G. Gregory

LIST OF TABLES

LIST OF ILLUSTRATIONS

TABLE OF CONTENTS (Cont'd)

DEVELOPMENT OF A SOLID-STATE IMAGE CONVERTER

by Carl T. Huggins

LIST OF ILLUSTRATIONS

PROPAGATION STUDIES

by Paul M. Swindall

TABLE OF CONTENTS (Concluded)

LIST OF ILLUSTRATIONS

HYDROGEN MASER RESEARCH ACHIEVEMENTS AT MSFC

By

John G. Gregory

SUMMARY

The basic principles and the construction of a hydrogen maser and its potential as a highly stable frequency reference for precision tracking systems are discussed. Improvements in stability and size are presented and future improvements are proposed. Results of measurements of relative frequency stability of two masers and the comparison of a hydrogen maser and a cesium beam are discussed. Also presented is the status of the hydrogen maser program and possible areas of application.

LIST OF SYMBOLS

Author

X - dimensionless measure of the external magnetic field, $X = \frac{\mu_e B_E}{\Delta W}$

I - quantum number related to the nuclear angular momentum

F - quantum number related to the total angular momentum of the entire atom

m_F - magnetic quantum number

μ_e - electronic dipole moment

B_E - external magnetic field

W - energy of the atom

I. INTRODUCTION

Tracking, communication, and guidance requirements for the launch, earth orbital, and deep space phases of a mission often demand highly stable frequency sources possessing a high order of short and long term frequency stability as well as a high degree of intrinsic reproducibility. Many tracking systems, such as MSFC's ODOP and command and communications system, use the doppler frequency for range measurements. Range rate measurements require a high order of short term stability; in range measurements the emphasis is placed upon long term stability.

More stringent requirements are placed upon long term stability when position data are required in addition to range and range rate data. Employing a three-station geometry and integrating the doppler frequency gives position as well as range data. The three station configuration requires that the doppler data obtained be referenced to a common, highly stable frequency source. This can be accomplished by transmitting a frequency reference from one station to the other two stations. Transmitting a stable frequency reference is undesirable because such transmission:

1. Is susceptible to variations caused by weather and atmospheric conditions.

2. Is a potential source of electromagnetic interference, particularly near the launch area.

3. Places limitations on the station geometry.

A solution to these problems would be to provide each station with its own frequency reference, whose instability would be a negligible factor in the determination of range, range rate, and position. In 1961, MSFC began a search for such a frequency source and found that the hydrogen maser, invented by Dr. Norman Ramsey of Harvard University, had excellent possibilities for providing long and short term stability. A contract was awarded to the Quantum Electronics Division of Varian Associates*, which had been working in the frequency control field with both hydrogen and cesium, to develop a hydrogen maser frequency source. The hydrogen maser

* Contract NAS 8-2604, principal experimenters are Dr. Robert Vessot and Dr. Jacques Vanier.

was chosen because it has the following desirable characteristics:

1. It has a narrow line width, resulting from atoms having a long interaction time in a very unperturbed condition.

2. Doppler shifts of the first order are very small because the average velocity of the atoms in the bulb is nearly zero.

3. Being a maser oscillator, the device has inherently low noise and avoids the disadvantages of electronic servos used to seek the center of the line.

II. BASIC THEORY

A hydrogen maser oscillator is a device which relies on three processes for successful operation:

1. Dissociation of molecular hydrogen into atomic hydrogen.

2. Selection of atoms of the proper energy state.

3. Storage of these atoms for a relatively long period of time.

A functional schematic diagram of the atomic hydrogen maser is given in Figure 1. Molecular hydrogen is dissociated by an electrical discharge and the atoms are formed into a beam. This beam contains atoms at various energy levels. Figure 2 shows the Zeeman splitting of the hyperfine energy levels of the ground electronic states of hydrogen. It is important to note that energy levels for which $m_F = 0$ leave the zero magnetic field axis with zero slope. Transitions between these levels afford the best opportunity for making highly stable frequency sources because the transition frequencies are least dependent upon fields arising from the environment.

The beam, containing hydrogen atoms in the various states, is passed through a state-selecting magnet where, by virtue of the differences in the effective atomic dipole moments, the upper pair of hyperfine levels are focused into a converging beam while the lower pair of hyperfine levels are deflected out of the beam (Fig. 2).

The beam containing the higher pair of hyperfine Zeeman states is passed into a specially-coated quartz storage bulb located inside an RF cavity. The atoms make random collisions with the walls of the coated bulb and are reflected. During this process,

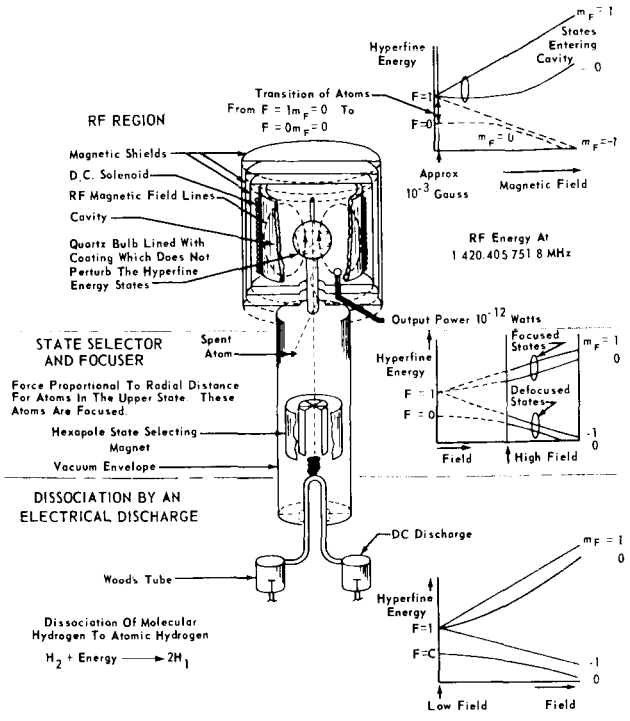

FIGURE 1., SCHEMATIC DIAGRAM OF THE HYDROGEN MASER

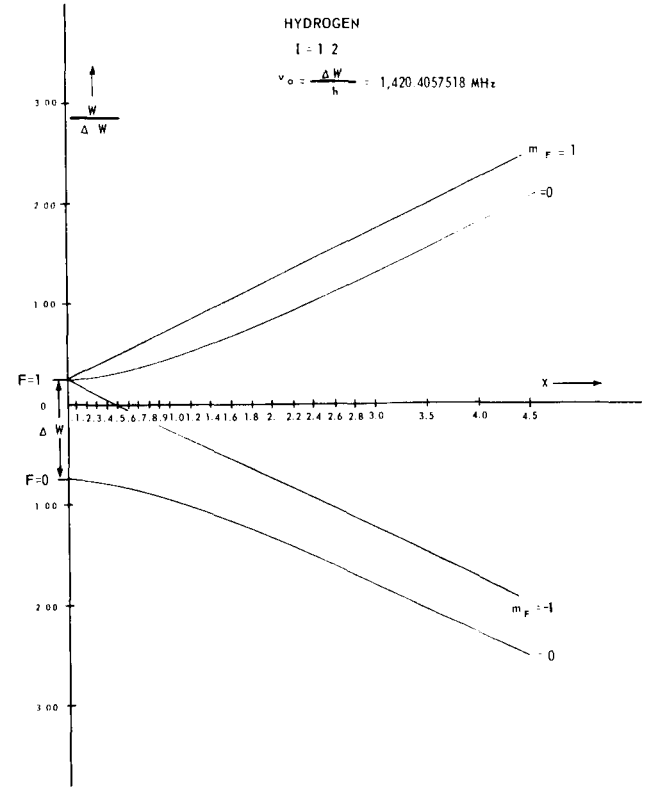

FIGURE 2. ZEEMAN ENERGY DIAGRAM FOR ATOMIC HYDROGEN

the atoms interact with the microwave field within the RF cavity which is tuned to the frequency of the hyperfine frequency of the $F = 1, m_F = 0 \rightarrow F = 0, m_F = 0$ transition. The interaction between the atoms and the microwave field continues until the atoms give up their energy usefully to the microwave field. Interaction periods in the order of one second have been achieved. The long interaction time permits coherent stimulation of the hydrogen atoms and sustained maser oscillation. This is detected by means of a small coupling loop. The power level available is approximately 10^{-12} watts.

The quartz storage bulb and the RF cavity are surrounded by three sets of magnetic shields and a set of coils, as shown in the upper part of Figure 1. The magnetic shields are used to reduce the ambient field. The coils are used to produce a small, uniform magnetic field whose component is along the beam axis for the purpose of separating the Zeeman levels to be sure only the $F = 1, m_F = 0$ states in the selected atoms contribute to the maser action. It is important to point out also that, except for atomic hydrogen, the space within the maser is evacuated and that provisions are made for removing the expended hydrogen.

III. DESCRIPTION OF A HYDROGEN MASER

Figure 3 is a schematic diagram of a hydrogen maser similar to the two which were built for MSFC. The base of the maser, which is about the size of a desk, houses the hydrogen supply, discharge assembly, vacuum system, and thermal and magnetic field controls. The upper portion is cylindrical, 82 cm long and 48 cm in diameter, containing the storage bulb, microwave cavity, magnetic field coils, thermal coils, and magnetic shields. Figure 4 shows an enlarged view of the upper portion of the maser. Figure 5 is a photograph of one of MSFC's masers undergoing tests.

Commercial grade hydrogen, stored in a small tank, is passed through a controlled leak into a palladium purifier and then to the discharge chamber (Figs. 3 and 4). The discharge chamber, approximately 2.5 cm in diameter and 2.5 cm long, is located between two RF coils resonated at 112 MHz (Fig. 6). A solid-state crystal-controlled oscillator generates 10 watts of power and produces a discharge in the gas which dissociates molecular

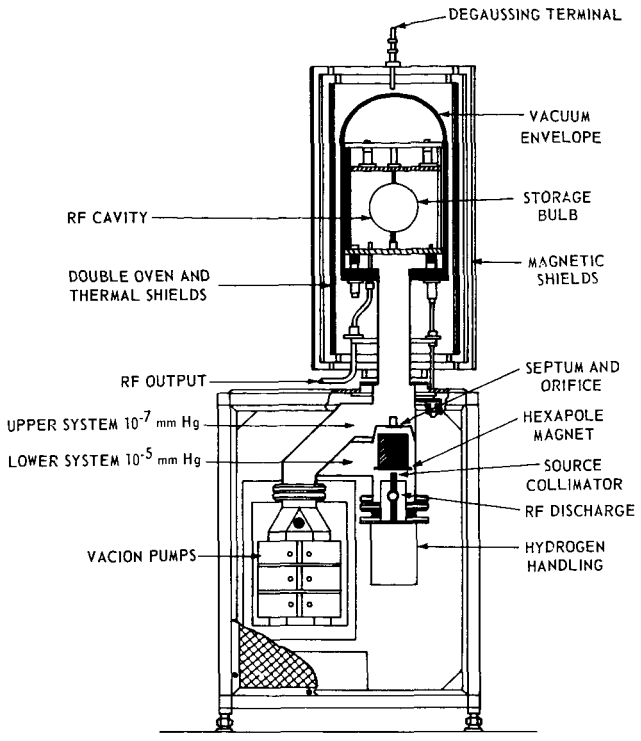

FIGURE 3. HYDROGEN MASER CUTAWAY

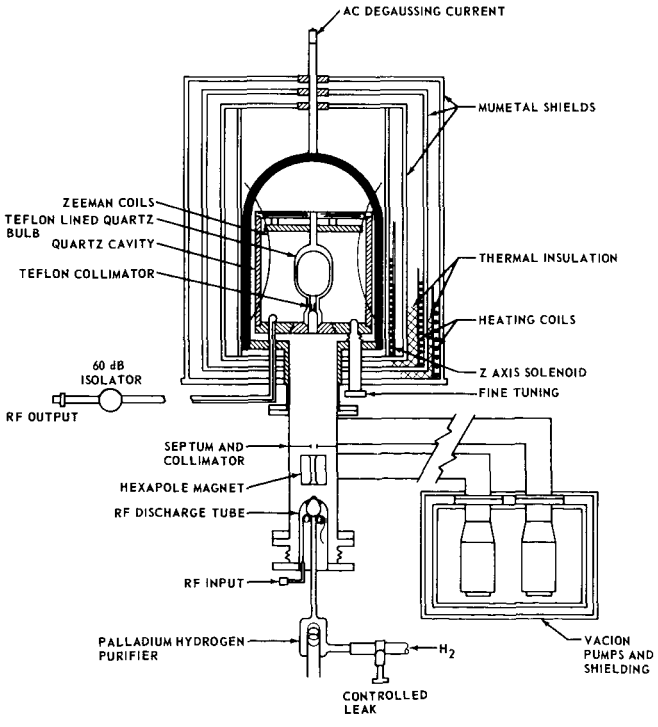

FIGURE 4. HYDROGEN MASER TOP ASSEMBLY

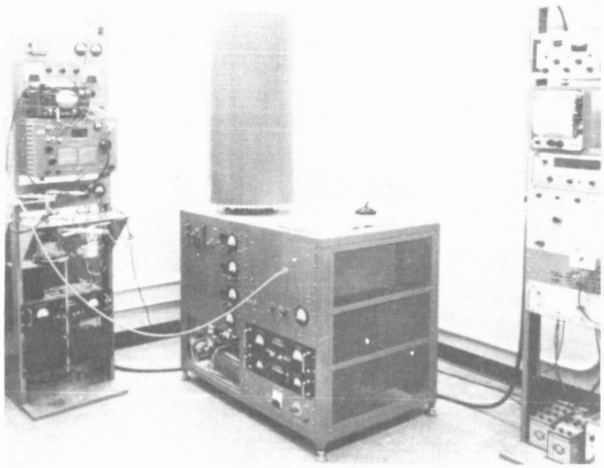

FIGURE 5. HYDROGEN MASER AT MSFC

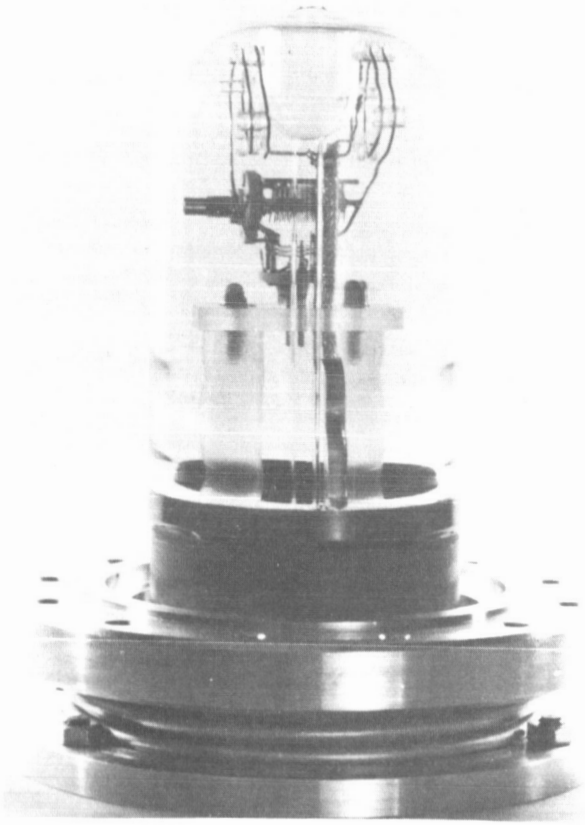

FIGURE 6. RF DISCHARGE SOURCE ASSEMBLY

hydrogen into atomic hydrogen. The pressure in the discharge can be set from 0.2 to 0.02 mm Hg. A beam of atoms is formed by allowing the atoms to escape through a multitube collimator having about 400 tubes, each tube averaging 0.038 mm in diameter with walls 0.005 mm thick. The collimator (Fig. 7) is approximately 1.4 mm in diameter and 1.4 mm long and is located at the output of the source. The collimator allows a total flux into the lower vacuum system of about 10^{16} atoms/s, so that a pressure of 10^{-5} mm Hg can be maintained by a VacIon pump with the maser in operation. The beam containing hydrogen atoms in selected states proceeds through a collimator to the upper vacuum chamber evacuated by another VacIon pump. The upper vacuum chamber, maintained at a pressure of 10^{-7} mm Hg, encloses the storage bulb and RF cavity. This prevents atmospheric disturbances from detuning the cavity. Also, differentially pumping the source and storage bulb chamber prevents excessive beam scattering.

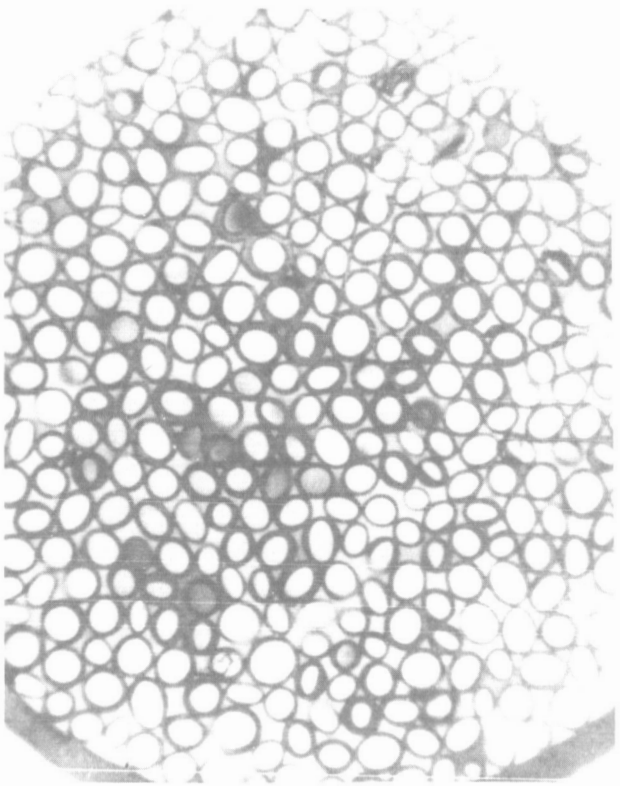

FIGURE 7. COLLIMATOR CROSS SECTION

The RF cavity (Fig. 8) is made of a fused quartz cylinder silvered on the inside and isolated from the bell jar with thin-walled quartz tubes. Having the cavity under vacuum in a bell jar provides a good thermal environment. The bell jar (Fig. 8) enclosing the cavity is made of copper and is welded to a copper base plate that contains the weld joints to the tuner and output coupling. Surrounding the bell jar assembly is a triple set of mumetal shields and a double oven built as one assembly. The inner oven is controlled

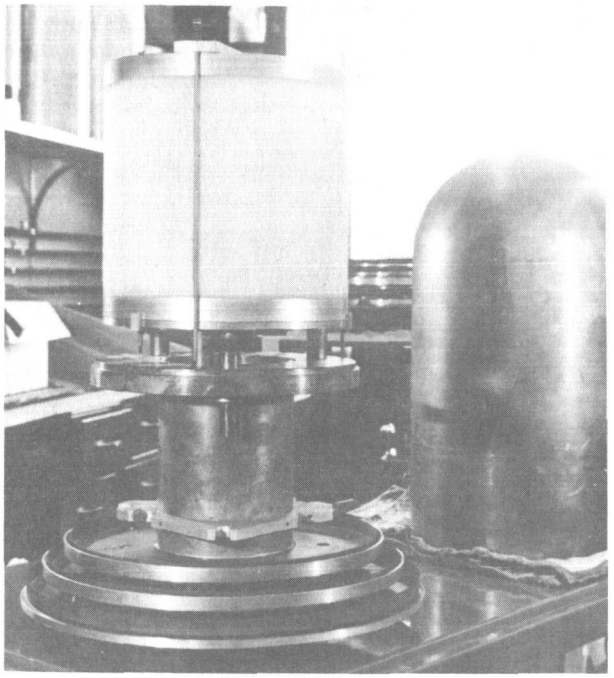

FIGURE 8. RF CAVITY ASSEMBLY

to 1/100 °C at a temperature of 40° C. The outer oven is set at 39° C. Cavity temperature is monitored by a platinum thermal bridge on the bell jar and controlled by an electronic servo system. The cavity mode is the cylindrical TE_{011} mode, which has only azimuthal wall currents; therefore, good contact between the cylinder and end plates is not required. The unloaded cavity resonates with a length and diameter equal to 27.6 cm. The theoretical Q is 87 000 for silver plated walls; however, in practice, a Q of 60 000 is obtainable. The quartz storage bulb does not appreciably affect the Q, but will decrease the resonant length of the cavity. To compensate for the peculiarities of the storage bulb, the position of one end plate is adjustable.

The quartz storage bulb is oval with a nominal diameter of 15 cm and is coated with teflon. Control of the lifetime of atoms in the bulb is obtained by the size of the bulb and by the size and flow factor of the collimator. Very simple collimators are made of solid teflon or by coating a pyrex plug and are seated like a stopper in the mouth of the bulb.

As a result of the quadratic field dependence of the desired transition, it is desirable to reduce the ambient field at the storage bulb to a very low value. The most satisfactory way to accomplish this is to use magnetic shields. Three concentric cylindrical mumetal shields reroute externally applied field lines away from the interior, and the inner shield forms a cylindrical equipotential surface for the fields generated by the interior solenoid. The solenoid is used to counteract the earth's magnetic field and to introduce a small uniform component along the beam axis for separating the Zeeman levels.

IV. FREQUENCY MEASUREMENTS

An extensive frequency stability measurement program was undertaken to determine the performance of the two masers developed for MSFC. The program consisted of measuring:

1. The relative long and short term stability of MSFC's two hydrogen masers.

2. The precision to which a given pair of masers can be reset with respect to frequency.

3. The ratio of cesium to hydrogen frequencies of hyperfine separation.

A very simple method for making frequency comparison measurements to determine the relative frequency stability between two masers is presented in Figure 9. The output from each maser is fed through an isolator providing 60 dB of isolation. The

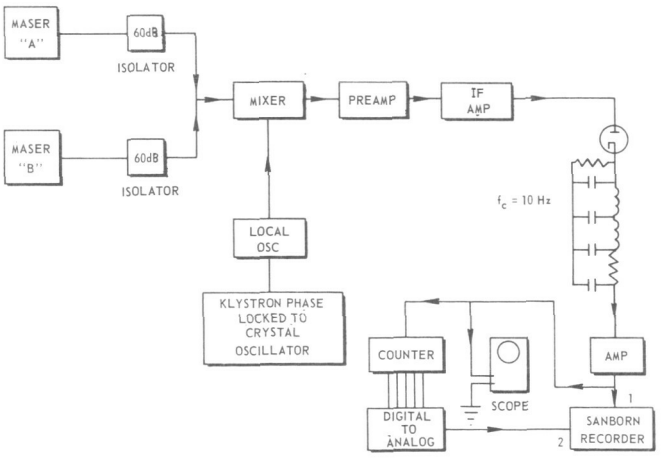

FIGURE 9. FREQUENCY COMPARISON RECEIVER

signals are then both connected to the input of a receiver consisting of an IF amplifier terminated in a diode. The output of the diode is filtered and fed to a strip chart recorder. The filtered signal also operates a counter that measures the beat period or the period for 10 beats. The counter is connected to a digital-to-analog converter whose output is also

recorded on the strip chart. Figure 10 is a sample of some of the initial measurements made on MSFC's two masers.

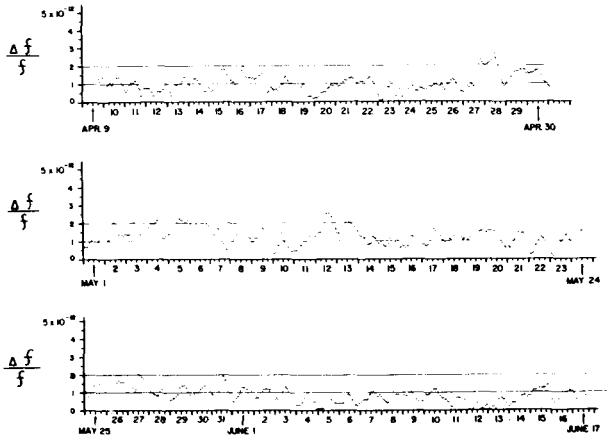

FIGURE 10. FREQUENCY DIFFERENCE BETWEEN TWO HYDROGEN MASERS

V. ACCOMPLISHMENTS

The maser program sponsored by MSFC has led to the design of the H-10 maser which represents the first step in reducing the size of the hydrogen maser. Figure 11 is a schematic diagram of the H-10, and Figure 12 is a photograph of a pair of H-10's in their final stages of completion. The H-10 maser is 56 cm square at the base, 200 cm high, and weighs about 360 kg. Improvements have been made in the vacuum system, thermal control system, and electronic packaging.

The following table lists the characteristics of the hydrogen maser achieved under MSFC's program with Varian Associates.

TABLE I. HYDROGEN MASER STABILITY

(rms deviation from the mean)

One second	5×10^{-13}
One minute	6×10^{-14}
One hour	3×10^{-14}
One day	2×10^{-14}
One month	3×10^{-13}
Resetability	$\pm 5 \times 10^{-13}$

Nominal Resonance Frequency 1420.405751 MHz

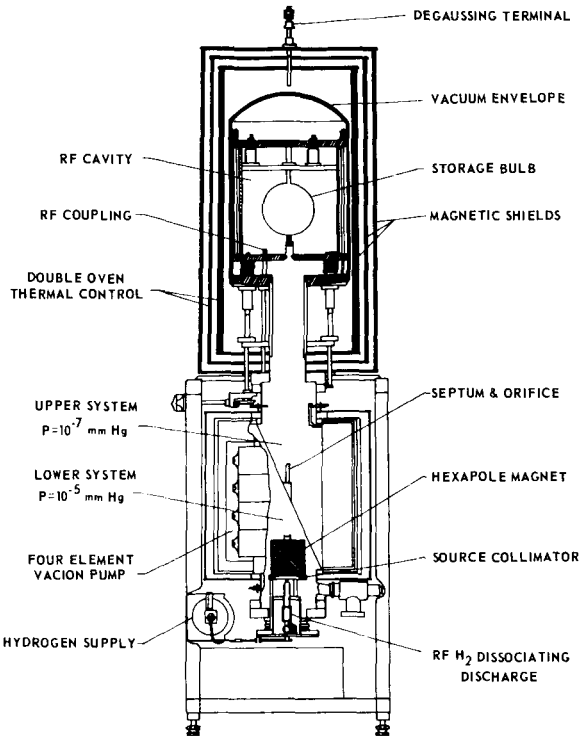

FIGURE 11. H-10 ATOMIC HYDROGEN FREQUENCY STANDARD

A program is underway to reduce the size of the present H-10 to approximately half. Investigations are being carried out with a spherical quartz dielectric cavity (Fig. 13). This cavity is considerably smaller than the cylindrical cavity now used and would allow a substantial reduction in the size of the magnetic and thermal shields. The quartz spherical cavity would be quite rugged and could be the first step in the design of a hydrogen maser for space application.

VI. APPLICATION

Hydrogen masers are presently being evaluated or are on order by various NASA centers, JPL, Harvard University, and the National Bureau of Standards (Boulder, Colorado). The hydrogen maser, because of its excellent long and short term frequency stability, is useful for laboratory time-frequency measurements, for spectroscopy, and as a frequency reference for precision tracking systems. These applications deal only with the ground based hydrogen maser. In space it may be applied in the area of geodetic research, navigation, time distribution, and important physical experiments such as the relativistic gravitational red shift.

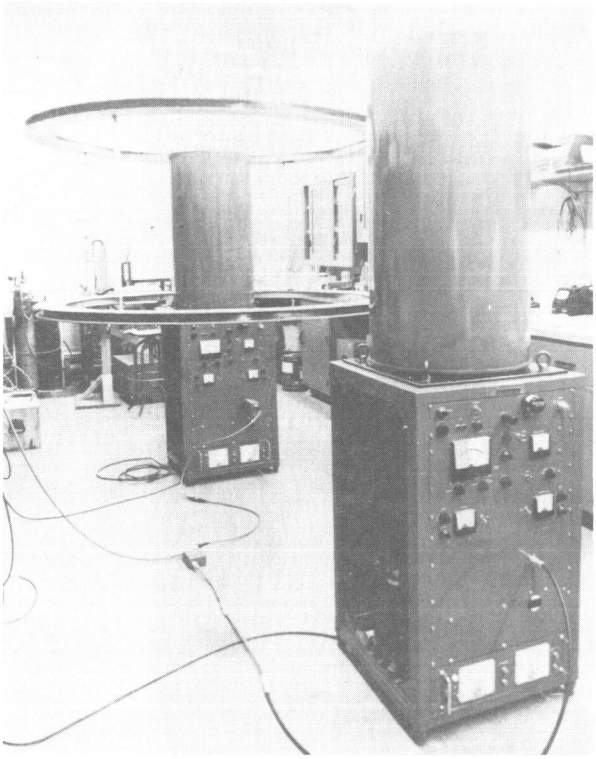

FIGURE 12. H-10 MASER ASSEMBLY COMPLETION

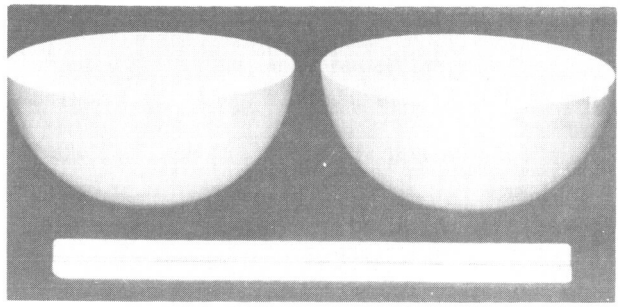

FIGURE 13. SPHERICAL QUARTZ CAVITY

BIBLIOGRAPHY

1. Vessot, R. F. C. and Peters, H. E.: The Design and Performance of an Atomic Hydrogen Maser. IRE Trans. Instr., vol. I-II, Dec. 1962, pp. 183-187.

2. Vessot, R. F. C.; Peters, H. E.; and Mueller, L: A Comparison of Performance Characteristics of Hydrogen, Thallium and Ammonia Masers. 1965 Proc. 19 Annual Frequency Control Symposium.

3. Vessot, R. F. C.: Frequency Stability Measurements Between Several Atomic Hydrogen Masers. Quantum Electronics III. P. Grivet and M. Bloembergen, Eds., Columbia UP (New York), 1964.

4. Vessot, R. F. C. and Peters, H. E.: Frequency Beat Experiments with Hydrogen Masers. 1963 Proc. 17 Annual Frequency Control Symposium.

5. McCoubrey, A. O.: Frequency Control by Microwave Atomic Resonance. The Microwave Journal, Nov. 1961.

6. McCoubrey, A. O.: A Survey of Atomic Frequency Standards. Proc. IEEE, special issue on Frequency Stability, pp. 116-135.

7. Ramsey, N.: Molecular Beams. Oxford Press (New York), 1956.

8. Kleppner, D., et al.: Hydrogen Maser Principles and Techniques. Phys. Rev., vol. 138, m. A972, 1965.

9. Singer, S. F.: Application of an Artificial Satellite to the Measurement of the General Relativistic Red Shift. Phys. Rev., vol. 104, No. 1, Oct. 1956.

DEVELOPMENT OF A SOLID - STATE IMAGE CONVERTER

By

Carl T. Huggins

SUMMARY

A solid-state image converter equivalent to the vidicon and capable of imaging radiation from the near infrared to 11 000 Å is discussed. The image converter and its associated circuit comprise a very small solid-state television camera designed for space use. A monolithic mosaic of phototransistor elements is complemented by densely packed integrated electronic circuits containing commutating switches, logic and switch-pulse generating circuits, and a video preamplifier (emitter follower amplifier).

I. INTRODUCTION

In 1960 and 1961, when the testing of tubes for television cameras for space use was begun, it was found that the operating environment was the most serious problem associated with the television system. Tests in 1960 through 1963 indicated that obtaining pictorial information by the use of conventional television imaging tubes was not the best electronic means. Conceivably a system operating on the basis of solid-state technology could ultimately provide the device for obtaining this pictorial information without having most of the objectional features of present standard and experimental cameras.

A system was envisioned in which the present imaging device, a conventional tube, would be replaced by a solid-state image converter operating on the basis of photoelectric effects and associated with circuitry using the most minute solid-state devices available. A program was outlined for development beginning in 1962 to produce as the ultimate goal a solid-state television camera compatible with standard television resolution and data rates.

Such a camera could then be improved to be compatible with our current closed-circuit systems for higher-resolution pictorial information transmission. This need not necessarily be for use with spaceborne cameras but could be used for other purposes such as data storage or conversion, or commercial use in sports, news, and educational broadcasting.

Ultimately, it is felt that this type of camera would be the one best suited for the extended space environment encountered on interplanetary missions. Because of the small size of this device, a number of them would occupy the same volume in a spacecraft as one standard flight television camera and consume equal or less power. Therefore, this device is directly related to the future planning of orbital, lunar, and planetary missions that may require the use of pictorial information. Since this camera, as well be explained later, uses digital logic in extracting information, it is applicable to any rate of readout. Its output could be transmitted over extremely narrow band or wide band RF links or over narrow band closed circuits such as telephone lines; but the circuit alterations necessary for this bandwidth change are extremely minor.

II. COMPLETE SYSTEM

The complete system in a 15.2 x 10.2 x 8.9 cm case is shown in Figure 1. The components of the camera are the mosiac sensor, the video preamplifier, the logic circuitry, and the commutating switches. Figure 2 shows the mosaic and supporting electronics. The silicon mosaic wafer is 1.3 cm square and utilizes a standard 16 mm lens system.

The readout circuitry packaged in the welded modules contains the required commutating switches, the logic and switch pulse generating circuits, and the video preamplifier (emitter follower amplifier) between the mosaic and the switches. These circuits permit high packing density since they are all molecular. Also included in the package are horizontal and vertical sweep generators and a video mixer amplifier. The power consumption is less than 4 watts.

A. MOSAIC SENSOR

The mosaic sensor is the solid-state equivalent of the vidicon and can image radiation in the visible

and near infrared regions to 12 000 Å. It is read out through a combination of metallized interconnections, bonded leads, and a printed circuit board instead of the beam-scan techniques employed by vidicon and image orthicon tubes.

Selection of material for the sensor was based on considerations of both reliable fabrication techniques and material spectral response. Silicon was selected to satisfy both conditions. To minimize cross talk, that is, to maximize isolation between the individual elements while maintaining high resolution, imaging is accomplished by conversion of light to current in discrete sensor regions, all of which are contained in a single monolith. The mosaic concept was introduced to achieve this large number of discrete isolated elements interconnected in a configuration in which each photo element could be sequentially interrogated as an isolated device without necessitating an unwieldy number of individual leads. The concept of XY interconnections was introduced to provide a structure both manageable in its number of leads and compatible with conventional viewing systems that accept XY data.

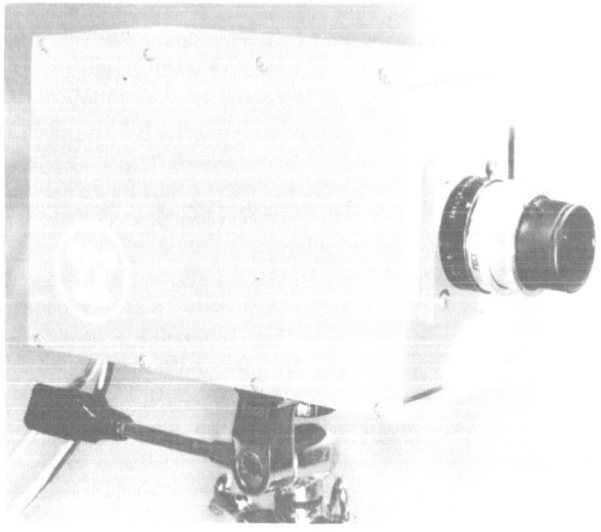

FIGURE 1. COMPLETE SOLID-STATE TELEVISION CAMERA

The mosaic sensor is a matrix of 50 x 50 NPN phototransistors on .254 mm centers, giving a total of 2500 phototransistors on a single monolith. Figure 3 shows a block diagram of the image converter.

The phototransistor elements have a square geometry with discrete emitter and base regions,

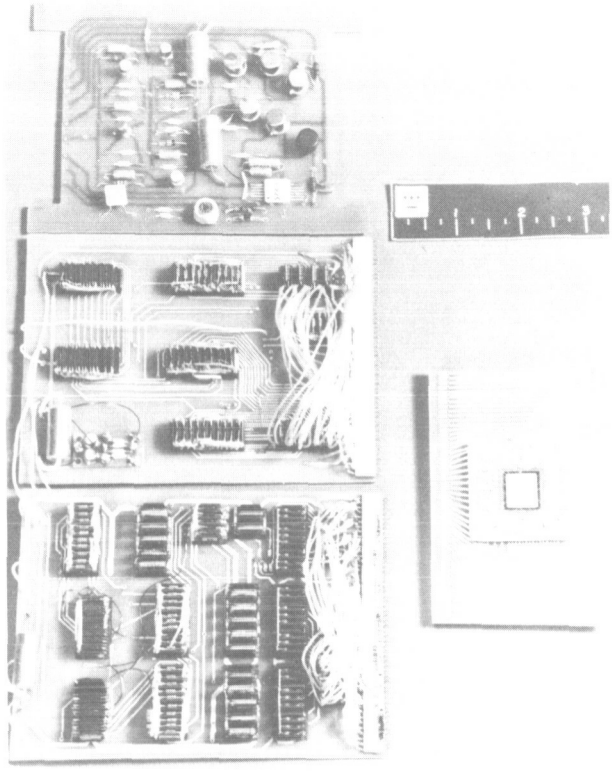

FIGURE 2. MOSAIC AND SUPPORTING ELECTRONICS

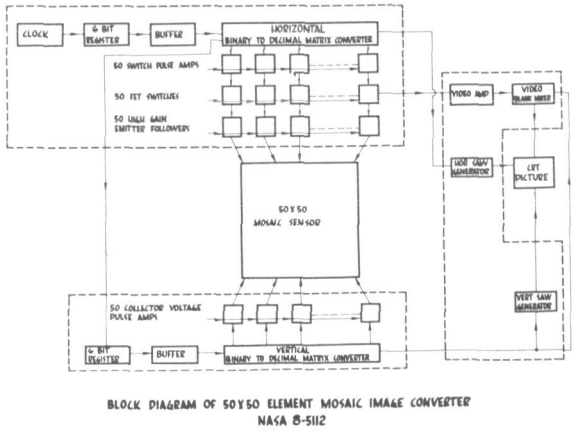

FIGURE 3. BLOCK DIAGRAM OF THE IMAGE CONVERTER

but with collector regions common to a column of 50 elements (Fig. 4). No electrical access is provided to the individual phototransistor base regions. The emitters are interconnected with evaporated aluminum strips in 50 isolated columns.

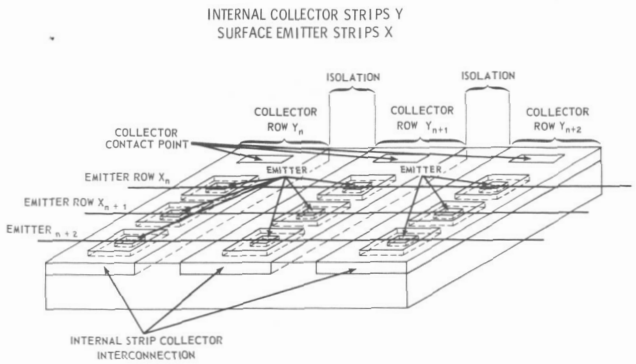

FIGURE 4. SECTION OF MOSAIC WITH XY INTERCONNECTIONS

Unique access to any individual element of the XY mosaic is available through one of the X and one of the Y external leads. Only the single element that lies at the intersection of these XY interconnections is interrogated.

Since a phototransistor structure was selected for the discrete photon detectors of which the mosaic is composed, the diffusion junction depths must be optimized with respect to photon absorption, surface recombination must be minimized, bulk minority carrier lifetime must be maximized, and the width of the depletion layer at the base collector junction must be large. Extreme processing control is not necessary to obtain useful single phototransistor elements; however, it is absolutely essential to fabricate a uniform mosaic of as many as 2500 elements.

This structure of light-sensitive elements with XY diffused and deposited interconnections is shown in Figure 5; the inset is an 8 x magnification.

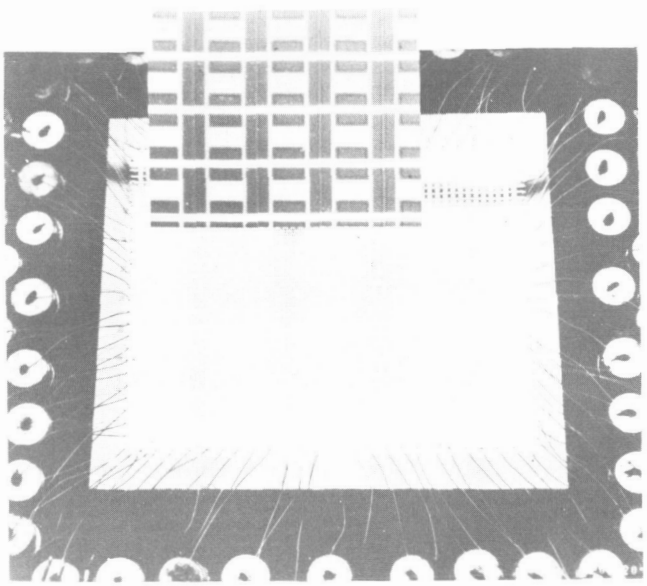

FIGURE 5. A 2500-ELEMENT MOSAIC

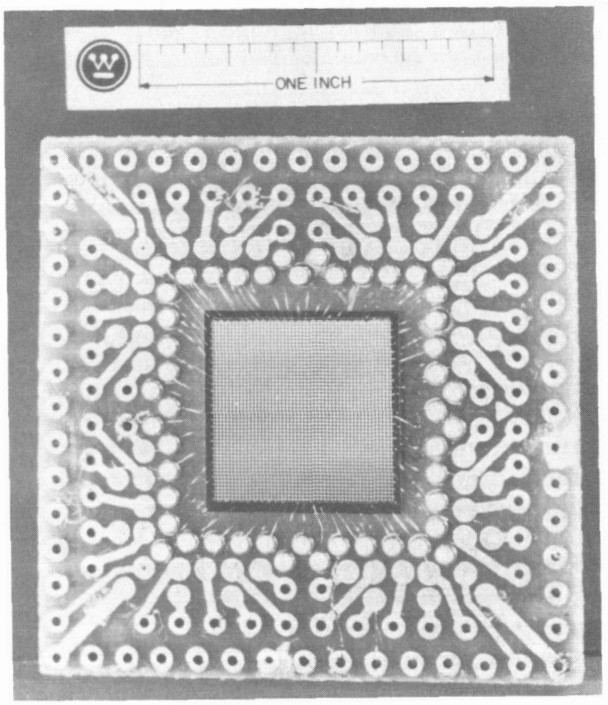

FIGURE 6. MOSAIC MOUNTED FOR TESTING

Figure 6 shows the mosaic mounted for testing.

B. VIDEO PREAMPLIFIER

Like a vidicon camera tube, a phototransistor element is a current generator and therefore requires a current amplifier, the gain required being substantial and depending on the level of light falling on the mosaic. To prevent noise from being generated by unwanted transients in the switch circuits, it is necessary to put the amplifier before the readout switch. The amplifiers in use now have a current gain of 300 at one microampere and an input impedance of 300 000 ohms. This allows operation in the linear area of the amplifier curve and produces sensitivity near that of the vidicon.

The video preamplifier (emitter follower amplifier) is necessary in the readout commutating circuitry for a number of reasons. The most important is that the impedance can be made much smaller so that switching speeds required to read out mosaics of much larger than 50 x 50 elements can be readily obtained.

C. LOGIC CIRCUITRY

Since clock frequencies approaching 1 MHz will ultimately be needed, flipflop binary logic was chosen because of its compatibility with integrated

molecular circuitry. From experience gained with diode matrix ring counting, it was decided to use standard NPN flipflop binary logic. Reliable operation of the flipflop was assured because of the sequential nature of the set/reset operation in the register of flipflops which divide the clock frequency and because of the nominal fan-out requirements. The logic provides the timing for pulsing the emitter readout switches, for application of voltage pulses to the collector rows of phototransistors, and for synchronizing the horizontal and vertical saw generators for the monitor.

The sampling switches multiplex 2500 mosaic analog signals onto one output resistance. Since there are 50 discrete elements on a line, the dwell time per element is about 6.6 μs and the clock frequency is 150 kHz. For the line switching, the dwell time is 50 elements times 6.6 μs, or 330 μs. The clock frequency for this sweep is synchronized with the element sweep, which is 3 kHz.

Readout is accomplished by applying a voltage to a 50-element collector strip and sequentially commutating the rows of emitter elements. In this way it is possible to read sequentially one element at a time while cutoff is maintained for all other elements.

The required timing for the series of 50 pulses to drive the 50-element commutator for both X readout and Y readout of the mosaic sensor is obtained from the 6-bit flipflop register. Since only 50 of the available 64 sequential outputs of the register are used, a carryover function or reset logic provision is necessary at the termination of readout of each line and row of mosaic sensor elements. This eliminates readout dead time. A diode matrix converter is used for translating each number to decimal notation. Amplifiers are needed at the output of the converter to provide correct amplitude and phase to drive each of the field-effect transistor switches. The Y readout logic is similar to the X readout logic, but it operates at a clock rate of only 3 kHz.

D. COMMUTATING SWITCHES

The sampling switches are now field-effect junction transistors so used as to provide excellent isolation between gate and source drained circuits, low noise level, and no offset voltage requirements. In addition, they require only one polarity-switching pulse. The signal handling capability of the switches ranges from 1 millivolt to 1 volt. These sampling switches multiplex 2500 mosaic analog signals onto one output resistance.

III. FUTURE PLANS

Present progress indicates that a more economical, compact, and reliable camera requiring less power can be made. As for its performance, we believe that the completion of the program will bring about better geometrical fidelity, greater dynamic range, less image smearing, and new types of signal processing with digital scanning. Of great importance to the lunar and planetary landing program is the fact that this is the only camera we know of that can be made completely sterile. The present contract period of performance is scheduled to produce a mosaic containing 100 x 128 elements. This will prove the feasibility of producing a mosaic containing 200 x 256 elements which is approximately equal to the resolution of the commercial home television receiver.

A second area of investigation is in coupling by means other than by wire. In this particular case, the one best adapted is the electro-optical coupling. As the number of elements increases, a method must be produced that will reduce the number of connections between the mosaic and the readout equipment. A 50 x 50 mosaic requires 100 connecting leads (Fig. 6), while a 200 x 256 mosaic will require 456 leads. Quantity production with this number of leads is considered highly impractical even if done by hand.

The program has, therefore, expanded into three areas instead of one: (1) processing improvements of the monolithic structure, (2) electro-optical coupling (this area must keep pace with the first or we are faced with an impractical interconnection problem), and (3) electronic peripheral timing and readout equipment, which requires a rate of time of operation increase that keeps pace with the element number increase in the monolith.

IV. CONCLUSIONS

The experimental results and the development of techniques to achieve them have proven that it is both feasible and practical to produce a solid-state camera equal in performance to an industrial camera. Its small power consumption, size, and weight plus its long life make it suitable for many uses in commerce, medicine, industry, and space. The work on this project was done by the Electronic Research Laboratory under the technical supervision of the author for NASA.

PROPAGATION STUDIES

By

Paul M. Swindall

SUMMARY

A method for increasing the accuracy of telemetry signal strength predictions is discussed. The systems considered are novel in that they have dc-to-20kHz signal strength recording responses. They make simultaneous phase coherent recordings of right circular, left circular, vertical, and horizontal polarizations. Research will continue in an effort to resolve propagation anomalies in preparation for manned vehicles.

I. INTRODUCTION

Accurate inflight signal strength measurements are necessary to verify the design and performance of RF and antenna systems. Such measurements may also be used to analyze the effect of rocket exhaust flames on the phase and amplitude of signals. Other propagation anomalies may be revealed by accurate signal strength information.

Because multipath propagation occurs normally at low altitudes when the signal level is high and appears as a low frequency periodic function, it will not be considered in this report.

II. TELEMETRY MEASUREMENTS

A. ANTENNA RADIATION

Antenna radiation patterns are a major factor in the transmission of data from the vehicle to ground stations. The patterns are developed and determined by scale modeling techniques, which must necessarily involve a number of assumptions, approximations, and simplifications. A reliable means for evaluating the accuracy of the antenna pattern scaling technique was needed.

B. RECORDING STATIONS

Field strength measurements on RF systems are made by the Atlantic Missile Range, but these measurements are secondary to data recording and are typically ± 5 to 6 dB in error and occasionally an order of magnitude in error. This is to be expected, since normally the automatic gain control (AGC) voltage of standard data receivers is used for signal strength recordings. This AGC voltage is logarithmic; and though it gives a wide dynamic range, it compresses the information, especially at high signal levels.

Other factors that limit the usefulness of the standard range recordings are:

(1) Early in the flights, the vehicle is close to the receiving stations and the receivers are near saturation.

(2) Frequency response is limited to a few cycles, or at best to a few hundred.

(3) Generally only one or two polarizations are recorded; four or more are needed for complete analysis.

Funds were requested for five specially instrumented stations. The amount approved permitted crude but accurate instrumentation of two vans.

A simple straightforward approach was used (Fig. 1); the best readily available commercial equipment was assembled inhouse with a minimum of modification. A manually tracked antenna, the most critical part of the system, was developed inhouse because of limited time and funds.

C. DESIGN REQUIREMENTS

To define the system performance completely requires all senses of polarization simultaneously; i.e., left circular, right circular, vertical, and

horizontal. In addition to steady state or low frequency response average signal information, instantaneous information was desirable to determine the noise characteristics imposed on the signal. The data on the signal are neglected and used only for identification. Some of the design goals were to have a recording of all polarizations, linear signal strength, wide frequency response, mobility, and the best obtainable accuracy. Higher frequencies are also needed for particular aspects of studies for which the data are now being used. The vans might possibly be converted to S-band for use with the UHF telemetry and the command and communication system on the Saturn V program.

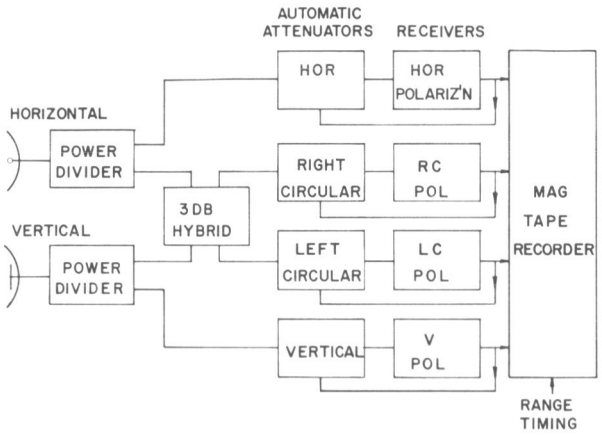

FIGURE 1. SIMPLIFIED BLOCK DIAGRAM OF RECEIVING STATION

These vans, specifically instrumented for signal strength measurement for complete analysis, are the only ones known to be in existence using the technique described here. They have been used to track vehicles other than Saturn, such as Atlas-Centaur, Polaris, and Titan, though the difficulty involved in automatic data handling has only recently been solved with a new computer program developed by the MSFC Computation Laboratory. Some minor improvements are being added to the stations for easier data handling and better compatibility. When these are completed, this computer program, as well as the reduced data, will be made available to interested people studying flame effects and other propagation effects.

III. PARABOLIC DISH ANTENNA

Figure 2 shows an antenna with a 3.05 m diameter parabolic reflector and a novel feed arrangement. The feed arrangement improves the side lobe structure, thus reducing the multipath data deterioration caused by ground reflection of the side lobes.

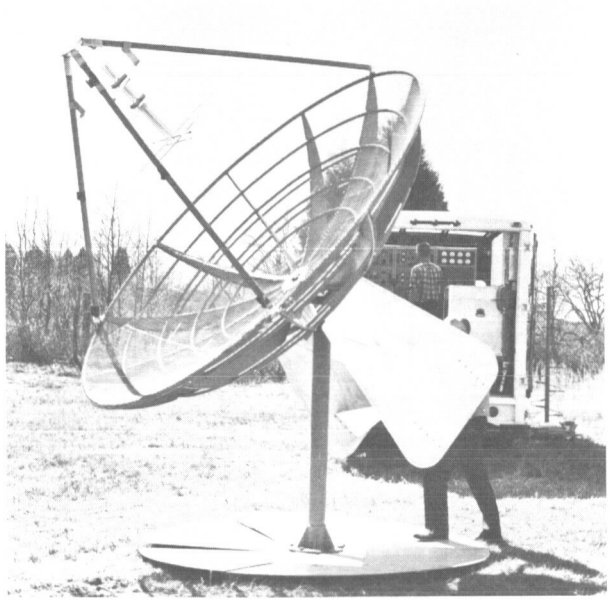

FIGURE 2. OVERALL VIEW OF PARABOLIC DISH, TURNSTILE ANTENNA

The turnstile element (Fig. 3) and the half wavelength reflector comprise a feed which has reduced side radiation. The phase center of the feed is apparently shifted nearer the ground plane and a considerable percentage of the power reradiated by the resonant reflector. This secondary radiation from the 1/2-wavelength reflector edges is cancelled at 90 deg because it has 180 deg phase difference perpendicular to the antenna lobe. This phenomenon reduced the first side lobe of the prototype 1/4-scale design from minus 10 or 12 dB to minus 15 or 16 dB. The feed was shifted off center, which reduced the radiation toward the ground 1 or 2 dB more. In the final full scale model, with careful focusing, the first side lobe was down 16 or 17 dB; all other side and back radiation was reduced 20 dB or more. The main lobe is a more accurate approximation of an ideal wedge shape than is normally accomplished.

The dual element or parasitic technique for impedance matching also served as a broadbanding device, increasing the useful turnstile bandwidth by a factor of three or more. The calculations in Figure 4 show the relations of mutual impedance of the parasitic element to the input impedance of one driven element of the reflector.

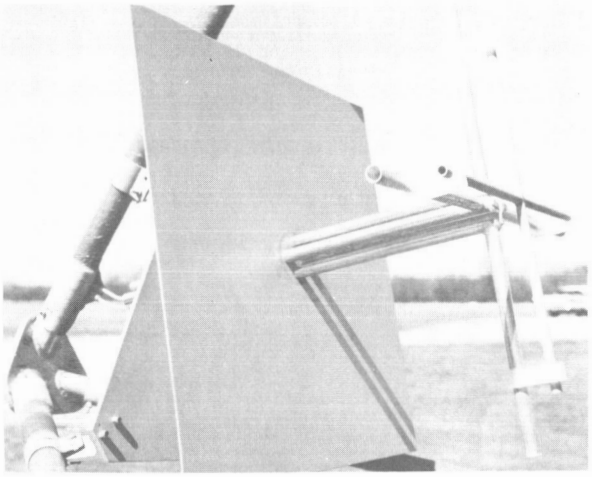

FIGURE 3. TURNSTILE ANTENNA IN PARABOLIC DISH

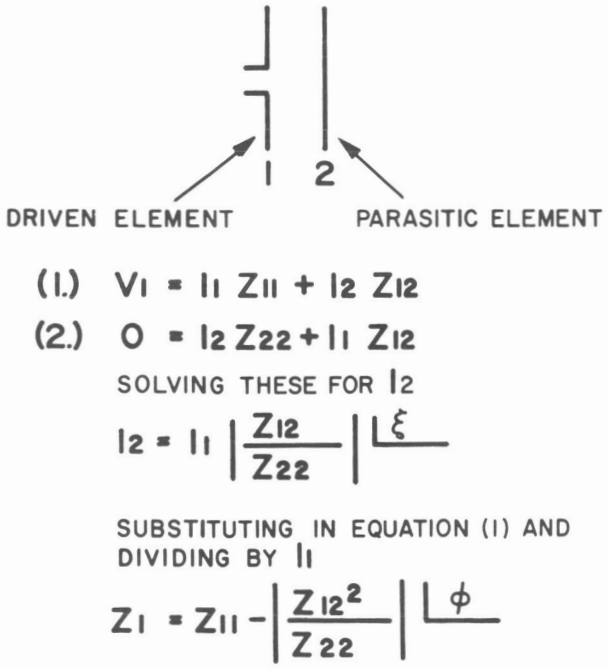

FIGURE 4. IMPEDANCE COMPENSATION

The signal from the antenna is fed into a 3-dB hybrid coupler where the circular components are derived (Fig. 5). Then, it feeds through the AGC step attenuators controlled by an output from the receivers. These attenuators either increase or decrease the sensitivity of the receivers in 10 dB increments, depending on the signal strength. The increments of 10 dB were chosen so that spurious or

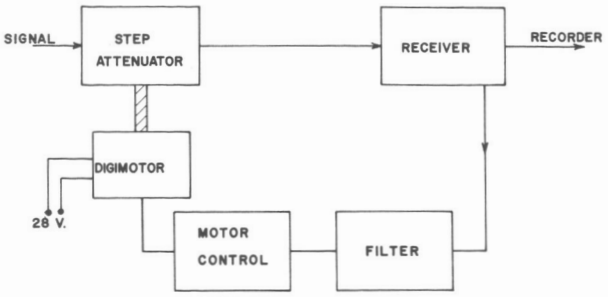

FIGURE 5. EXTERNAL AUTOMATIC GAIN CONTROL LOOP

transient fluctuations in the signal would cause minimum loss in data and yet keep the receivers in their most linear range. Though loss of data occurs during switching (approximately 6 ms), this method eliminates errors normally associated with conventional receiver AGC and transient response.

Figure 6 shows the van and antenna as they were shipped to the Cape; Figure 7 shows the controls in the van. Each van was made portable and mobile

FIGURE 6. TRACKING VAN AND ANTENNA

with self-contained power generators and WWV receivers to monitor time signals from the National Bureau of Standards. They could be operated without external power or range timing if necessary, though power and timing have been available at all sites.

IV. DATA

A. DATA REDUCTION

A major problem was that no technique was available for automatically reducing the data and

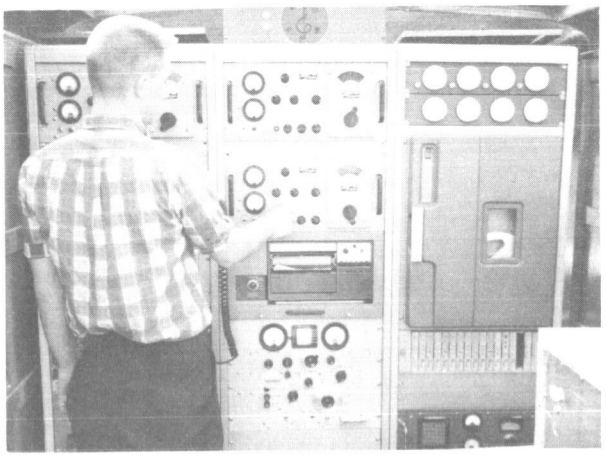

FIGURE 7. CONTROLS IN PROPAGATION STUDIES VAN

only typical small samples of a few seconds interval could be reduced manually. The early part of the project yielded only manually extracted average data except for particular times when exact retro-rocket firing time, ullage firing time, or stage separation could be identified by the effect of the functions on the signal.

B. COMPUTER PRINTOUT

The tapes were then used in establishing a computer technique to automatically reduce the flame data. The digital technique yields data at 10 ms intervals with a 1kHz response. The equations involved in the solution of the angle of the polarization ellipse (r) are shown in Figure 8.

The computer printout (1) gives a sample of the data corrected for calibration for each sense of polarization, (2) contains the calculated angle of the polarization ellipse (Fig. 9, equation 1), (3) contains calculations of the validity of the data (Fig. 9, equations 2 and 4), and (4) gives a go/no-go indication in one column to show if the data are good or bad. In other words, with the four simultaneously received phase-related signals, one receiver channel can be checked against the others. As indicated, equation 4 must always equal 1; any deviation from 1 indicates errors in one or more of the polarizations. In the case of an excessive constant deviation from 1, the final data accuracy can be improved by inserting a constant correction in one or more polarization calibrations. The limit for ± 1 dB error is 0.6 to 1.3. Figure 10 shows a sample computer

$$E_x\angle 0^\circ,\ E_y\angle\phi^\circ \rightarrow \text{HYBRID COUPLER} \rightarrow E_R = .707\left[E_x\angle 0^\circ + E_y\angle\phi+90^\circ\right],\ E_L = .707\left[E_x\angle\phi^\circ + E_y\angle\phi^\circ\right]$$

$$E_R = .707\left[E_x + E_y(\cos\phi + j\sin\phi + 90^\circ)\right]$$

$$E_R = .707\left[E_x + E_y\sin\phi + j\,E_y\cos\phi\right]$$

$$E_L = .707\left[E_y\cos\phi + jE_x + E_y\sin\phi\right]$$

1. $2E_R^2 = E_x^2 + E_y^2 - 2E_xE_y\sin\phi$
2. $2E_L^2 = E_x^2 + E_y^2 + 2E_xE_y\sin\phi$

BY COMBINING 1. AND 2. $\sin\phi = \dfrac{E_L^2 - E_R^2}{2E_xE_y}$

$$r = 1/2\ \text{ARCTAN}\ \frac{2E_xE_y\cos\phi}{E_x^2 - E_y^2}$$

$$\cos\phi = \frac{\sqrt{(2E_xE_y)^2 - (E_L^2 - E_R^2)}}{2E_xE_y}$$

$$r = 1/2\ \text{ARC COS}\ \frac{E_x^2 - E_y^2}{2E_LE_R}$$

FIGURE 8. MATHEMATICAL ASPECTS OF ACQUIRING ALL POLARIZATIONS

1. $r = 1/2\ \cos^{-1}\dfrac{E_x^2 - E_y^2}{E_L\,E_R}$

2. $\dfrac{1}{\text{AXIAL RATIO}} = \dfrac{E_R^2 - E_L^2}{E_R^2 + E_L^2}$ $\quad -1 \leq \dfrac{1}{AR} \leq +1$

3. $PF = \dfrac{E_R^2}{E_R^2 + E_L^2}$ PERCENTAGE OF POWER IN RIGHT CIRCULAR COMPONENT

4. $A = \dfrac{E_x^2 + E_y^2}{E_L^2 + E_R^2}$ SHOULD ALWAYS EQUAL ONE

FIGURE 9. CHECK EQUATIONS

printout of the tabulated data, and Figure 11 shows a sample of an analog recording displaying the step functions in the data generated by the external 10 dB AGC attenuators.

C. ACCURACY

In the design of the receiving system, all errors were kept to a minimum practicable. A conservative receiving system relative accuracy of ± 1 dB included calibration error and circularity error in the receiving antenna. Absolute error is more dependent upon absolute calibration of the calibration generator, absolute gain of the antenna, and other absolute measurements. A conservative estimate of the accuracy of the overall receiving station is approximately ± 2 dB.

SPØNSØR BILLY R. PAGE R-CØMP-RRM ØRIGINATØR W. H. SWØRTWØØD R-CØMP-GE

PØLARIZATIØN PRØBLEM

TIME	EH	RH	EV	RV	EL	RL	ER	RR	EQ. 1 1/AR	EQ. 2 PR	EQ. 3 L	EQ. 4	ERRØR	CØUNTS HIGH
92.402	0.000630	4	0.000336	4	0.000316	3	0.000686	3	0.370	0.825	0.429	0.893	0	0
92.412	0.000660	4	0.000333	4	0.000301	3	0.000692	3	0.393	0.840	0.340	0.960	0	0
92.422	0.000677	4	0.000345	4	0.000328	3	0.000736	3	0.383	0.834	0.396	0.889	0	0
92.432	0.000643	4	0.000339	4	0.000292	3	0.000719	3	0.423	0.859	0.390	0.876	0	0
92.442	0.000664	4	0.000345	4	0.000306	3	0.000711	3	0.398	0.844	0.369	0.934	0	0
92.452	0.000647	4	0.000342	4	0.000316	3	0.000707	3	0.382	0.833	0.415	0.893	0	0
92.462	0.000643	4	0.000328	4	0.000297	3	0.000651	3	0.374	0.828	0.328	1.018	0	0
92.472	0.000656	4	0.000333	4	0.000328	3	0.000692	3	0.356	0.816	0.397	0.923	0	0
92.482	0.000664	4	0.000325	4	0.000301	3	0.000702	3	0.399	0.844	0.327	0.937	0	0
92.492	0.000639	4	0.000339	4	0.000306	3	0.000656	3	0.363	0.821	0.377	0.998	0	0
92.502	0.000609	4	0.000328	4	0.000301	3	0.000686	3	0.390	0.838	0.440	0.851	0	0
92.512	0.000647	4	0.000342	4	0.000301	3	0.000697	3	0.396	0.842	0.385	0.930	0	0
92.522	0.000686	4	0.000333	4	0.000316	3	0.000715	3	0.387	0.837	0.327	0.950	0	0
92.532	0.000664	4	0.000328	4	0.000301	3	0.000681	3	0.387	0.836	0.311	0.988	0	0
92.542	0.000656	4	0.000336	4	0.000306	3	0.000697	3	0.389	0.838	0.367	0.937	0	0
92.552	0.000639	4	0.000333	4	0.000306	3	0.000661	3	0.367	0.823	0.374	0.978	0	0
92.562	0.000668	4	0.000322	4	0.000292	3	0.000666	3	0.391	0.839	0.243	1.041	0	0
92.572	0.000647	4	0.000333	4	0.000311	3	0.000635	3	0.342	0.806	0.339	1.059	0	0
92.582	0.000651	4	0.000322	4	0.000292	3	0.000692	3	0.407	0.849	0.326	0.937	0	0
92.592	0.000625	4	0.000336	4	0.000297	3	0.000681	3	0.393	0.841	0.407	0.912	0	0
92.602	0.000630	4	0.000328	4	0.000297	3	0.000661	3	0.380	0.832	0.370	0.961	0	0
92.612	0.000647	4	0.000333	4	0.000287	3	0.000681	3	0.407	0.849	0.332	0.970	0	0
92.622	0.000647	4	0.000336	4	0.000306	3	0.000719	3	0.403	0.847	0.402	0.870	0	0
92.632	0.000664	4	0.000333	4	0.000271	3	0.000635	3	0.401	0.846	0.146	1.158	0	0
92.642	0.000630	4	0.000330	4	0.000292	3	0.000671	3	0.394	0.841	0.373	0.945	0	0
92.652	0.000643	4	0.000322	4	0.000297	3	0.000702	3	0.406	0.849	0.366	0.890	0	0
92.662	0.000664	4	0.000316	4	0.000287	3	0.000661	3	0.395	0.841	0.225	1.043	0	0
92.672	0.000620	4	0.000322	4	0.000297	3	0.000676	3	0.390	0.839	0.399	0.894	0	0
92.682	0.000639	4	0.000330	4	0.000287	3	0.000651	3	0.388	0.837	0.322	1.023	0	0
92.692	0.000651	4	0.000328	4	0.000292	3	0.000692	3	0.407	0.849	0.333	0.944	0	0
92.702	0.000634	4	0.000314	4	0.000292	3	0.000630	3	0.367	0.823	0.299	1.039	0	0
92.712	0.000643	4	0.000330	4	0.000297	3	0.000651	3	0.374	0.828	0.332	1.022	0	0
92.721	0.000639	4	0.000330	4	0.000306	3	0.000635	3	0.349	0.811	0.348	1.040	0	0
92.731	0.000639	4	0.000328	4	0.000287	3	0.000618	3	0.366	0.823	0.279	1.111	0	0
92.741	0.000647	4	0.000336	4	0.000287	3	0.000651	3	0.388	0.837	0.305	1.052	0	0
92.751	0.000620	4	0.000333	4	0.000287	3	0.000686	3	0.411	0.851	0.403	0.894	0	0
92.761	0.000647	4	0.000316	4	0.000292	3	0.000651	3	0.381	0.833	0.287	1.020	0	0
92.771	0.000625	4	0.000325	4	0.000301	3	0.000686	3	0.390	0.838	0.406	0.882	0	0
92.781	0.000639	4	0.000328	4	0.000297	3	0.000686	3	0.397	0.843	0.370	0.921	0	0
92.791	0.000651	4	0.000322	4	0.000297	3	0.000711	3	0.411	0.852	0.353	0.889	0	0
92.801	0.000660	4	0.000314	4	0.000282	3	0.000692	3	0.401	0.857	0.263	0.957	0	0
92.811	0.000647	4	0.000322	4	0.000292	3	0.000640	3	0.374	0.828	0.283	1.055	0	0
92.821	0.000656	4	0.000316	4	0.000292	3	0.000661	3	0.387	0.837	0.272	1.015	0	0
92.831	0.000643	4	0.000316	4	0.000292	3	0.000686	3	0.404	0.847	0.336	0.922	0	0
92.841	0.000647	4	0.000333	4	0.000306	3	0.000676	3	0.377	0.830	0.367	0.962	0	0
92.851	0.000651	4	0.000316	4	0.000297	3	0.000635	3	0.363	0.821	0.267	1.067	0	0
92.861	0.000656	4	0.000316	4	0.000297	3	0.000686	3	0.397	0.843	0.313	0.947	0	0
92.871	0.000639	4	0.000325	4	0.000301	3	0.000666	3	0.377	0.830	0.359	0.960	0	0

FIGURE 10. SAMPLE COMPUTER PRINTOUT

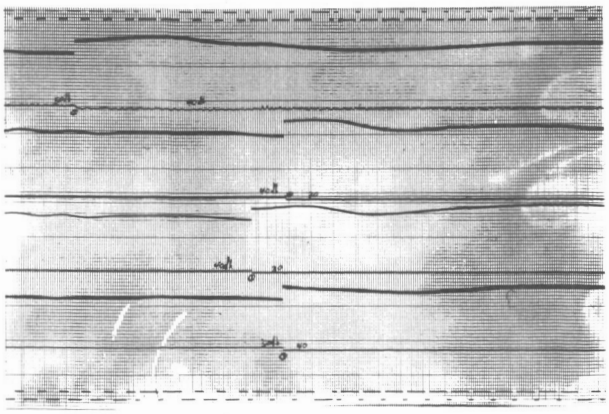

FIGURE 11. SAMPLE ANALOG RECORDING

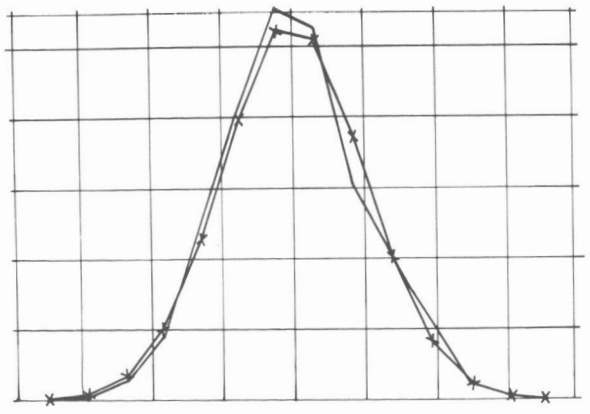

FIGURE 12. GAUSSIAN DENSITY COMPARED WITH MEASURED DENSITY

D. SA-10 NOISE SPECTRUM

Figure 12 shows the noise power spectrum plotted from data received on Saturn I, vehicle SA-10, during retrorocket firing. This curve shows that the noise spectrum is generally normal or Gaussian. The only deviation, which appeared at particular times during preliminary analysis, is a resonance effect from the reinforcement and cancellation (acoustical interference pattern) caused by

the clustering of engines. This resonance tends to peak the flame modulation, and therefore the signal, at certain frequencies.

Observations indicate a possible acoustic resonance modulation effect on the flame that appears as a shaping or peaking of the noise distribution curve at the acoustic resonance. This has not been completely substantiated but an effect has been observed that can be explained by this phenomenon. This effect approximates the resonant frequency of the engine or rocket nozzle in question.

E. FLAME ATTENUATION CONTOURS

Figure 13 shows a typical plot of predicted flame attenuation contours at Cape Kennedy for different vehicle altitudes. These are projected from a ray drawn from a vehicle antenna tangent to the inviscid boundary of the plume. Because they are mobile, the receiving stations can be placed at optimum locations to obtain data for comparison of actual and predicted flame attenuation. Figure 14 shows this comparison on SA-10, identifying the first and maximum flame effects and recovery. The smooth lines are predicted data and the plotted points are actual measurements; it can be seen that some error in the predictions is present. These and future measurements will be used to improve the accuracy of later predictions.

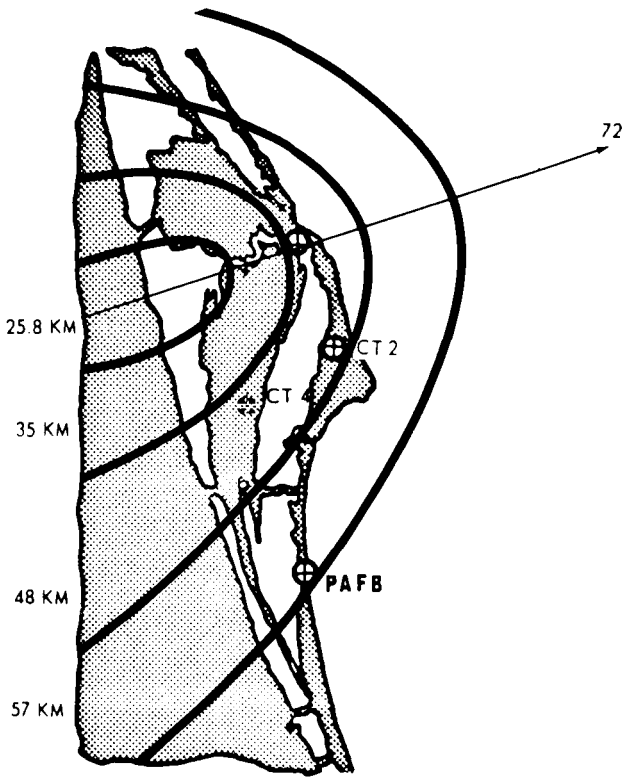

FIGURE 13. PREDICTED FLAME ATTENUATION CONTOURS FROM S-IC MAINSTAGE ENGINES

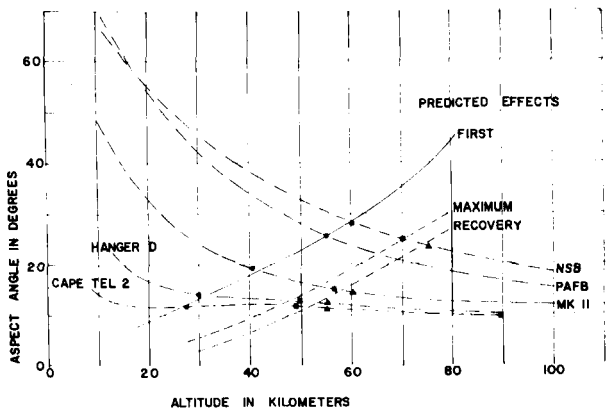

FIGURE 14. ACTUAL AND PREDICTED FLAME ATTENUATION

V. CONCLUSIONS

This research effort should continue, possibly with more emphasis on retaining or improving tracking, recording, and calibration accuracy. The information gathered will continue to be useful until the critical propagation anomalies are completely resolved in preparation for manned vehicles.

Another particularly important function of these receiving stations will be recording signal strength in the planned orbital antenna pattern experiment, in which the vehicle will be rolled to perform a more complete analysis of full scale antenna patterns.

APPROVAL

RESEARCH ACHIEVEMENTS REVIEW NO. 18

By John G. Gregory, Carl T. Huggins, and Paul M. Swindall

The information in these reports has been reviewed for security classification. Review of any information concerning Department of Defense or Atomic Energy Commission programs has been made by the MSFC Security Classification Officer. These reports, in their entirety, have been determined to be unclassified.

These reports have also been reviewed and approved for technical accuracy.

W. Haeussermann

W. HAEUSSERMANN
Director, Astrionics Laboratory

MSFC INTERNAL

DIR	1
DEP-T	1
DEP-A	1
AST-P	1
CC	1
CC-P	1
LR	1
MA-S	1
PA	2
E-DIR	6
F& D-CH	1
R-DIR	3
R-S	1
R-TS	1
R-AS	5
R-AERO (Through Branch Level)	30
R-AERO-T	9
R-ASTR	25
R-EO-R (Reserve)	50
R-COMP (Through Branch Level)	10
R-COMP-T	5
R-ME (Through Branch Level)	21
R-RP (Through Branch Level)	8
R-P& VE (Through Branch Level)	79
R-QUAL (Through Branch Level)	26
R-QUAL-T	8
R-TEST (Through Branch Level)	12
R-EO-DIR	
Dr. Johnson	1

MSFC INTERNAL (Cont'd)

LVO	2
I-DIR	1
I-I/IB-MGR (Through Branch Level)	10
I-V-MGR (Through Branch Level)	10
I-E-MGR	3
I-MICH-MGR	20
I-MT-MGR	2
MS-T	25
MS-IP	2
MS-IL	8
MS-I, Daniel Wise	1
Air Force Space Systems Division Huntsville, Alabama	1

NASA HEADQUARTERS

Dr. Mac C. Adams, Code R, Washington, D. C.	1
Mr. Milton B. Ames, Jr., Code RV, Washington, D. C.	1
Mr. Walter Beckwith, Code MTP, Washington, D. C.	1
Dr. Raymond L. Bisplinghoff, Code A, Washington, D. C.	1
Mr. Edmond C. Buckley, Code T, Washington, D. C.	1
Mr. Oliver Bungardner, Code MLT, Washington, D. C.	1
Mr. Roland H. Chase, Code RET, Washington, D. C.	1
Mr. Fred J. DeMeritte, Code RV-1, Washington, D. C.	1
Mr. Robert W. Dunning, Code RBA, Washington, D. C.	1
Dr. James B. Edson, Code R-1, Washington, D. C.	1
Mr. Albert J. Evans, Code RA, Washington, D. C.	1
Mr. Harold B. Finger, Code RN, Washington, D. C.	1
Mr. W. Foster, Code SM, Washington, D. C.	1
Mr. Robert Freitag, Code MC, Washington, D. C.	1
Mr. Edward Z. Gray, Code MT, Washington, D. C.	1
Dr. John Holloway, Code SC, Washington, D. C.	1
Maj. Gen. David M. Jones, Code MD-P, Washington, D. C.	1
Dr. Walton L. Jones, Code RB, Washington, D. C.	1
Dr. Hermann H. Kurzweg, Code RR, Washington, D. C.	1
Mr. William E. Lilly, Code MP, Washington, D. C.	1
Dr. Douglas R. Lord, Code MTS, Washington, D. C.	1
Mr. Ivan Mason, Code MAT, Washington, D. C.	1
Dr. George E. Mueller, Code M, Washington, D. C.	1
Mr. John F. Stearns, Code ATS, Washington, D. C.	1
Mr. T. T. Neill, Code RTR, Washington, D. C.	1

NASA HEADQUARTERS (Cont'd)

Mr. Joseph L. Murphy, Code KR, Washington, D. C.	1
Mr. Boyd C. Myers, Code RD, Washington, D. C.	1
Dr. J. Naugle, Code SG, Washington, D. C.	1
Dr. Homer E. Newell, Code S, Washington, D. C.	1
Mr. E. O. Pearson, Jr., Code RV-1, Washington, D. C.	1
Maj. Gen. Samuel C. Phillips, Code MA, Washington, D. C.	1
Mr. Maurice J. Rafferspergers, Code MTE, Washington, D. C.	1
Mr. Melvin G. Rosche, Code RV-2, Washington, D. C.	1
Mr. Charles T. D'Aiutolo, Code RV-1, Washington, D. C.	1
Mr. J. Warren Keller, Code RV-1, Washington, D. C.	1
Mr. J. L. Sloop, Code RC, Washington, D. C.	1
Mr. S. M. Smolensky, Code MCD, Washington, D. C.	1
Mr. Frank J. Sullivan, Code RE, Washington, D. C.	1
Mr. William B. Taylor, Code MT, Washington, D. C.	1
Dr. M. Tepper, Code SF, Washington, D. C.	1
Mr. Adelbert Tischler, Code RP, Washington, D. C.	1
Mr. Theofolus Tsacoumis, Code RET, Washington, D. C.	1
Mr. Gene A. Vacca, Code REI, Washington, D. C.	1
Dr. John M. Walker, Code RET, Washington, D. C.	1

CENTERS

Mr. H. Julian Allen, Director NASA, Ames Research Center Moffett Field, California 94035	2
Dr. Kurt H. Debus, Director NASA, John F. Kennedy Space Center Kennedy Space Center, Florida 32899	2
Mr. Paul F. Bikle, Director NASA, Flight Research Center P. O. Box 273 Edwards, California 93523	2
Dr. John Clark, Acting Director NASA, Goddard Space Flight Center Greenbelt, Maryland 20771	1
Dr. William H. Pickering, Director NASA, Jet Propulsion Laboratory 4800 Oak Grove Drive Pasadena, California 91103	2
Dr. Floyd L. Thompson, Director NASA, Langley Research Center Langley Station Hampton, Virginia 23365	2
Mr. N. E. Devereux **Library Supervisor** **NASA, Jet Propulsion Laboratory** **4800 Oak Grove Drive** **Pasadena, California 91103**	1

CENTERS (Cont'd)

Dr. Abe Silverstein, Director NASA, Lewis Research Center 21000 Brookpark Road Cleveland, Ohio 44135	2
Mr. Warren Gillespie Code EA 5 NASA, Manned Spacecraft Center Houston, Texas 77001	15
Mr. J. P. Claybourne, EDV-4 Chief, Future Studies Office NASA, John F. Kennedy Space Center Kennedy Space Center, Florida 32899	1
Mr. James Elms NASA, Electronics Research Center 575 Technology Square Cambridge, Massachusetts 02139	2
Mr. A. R. Lawrence Management Analysis NASA, Electronics Research Center 575 Technology Square Cambridge, Massachusetts 02139	25
Mr. John Boyd, Technical Assistant Office of Assistant Director for Astronautics NASA, Ames Research Center Moffett Field, California 94035	1
Mr. Chesley H. Looney, Jr., Ass't Chief Advanced Development Division NASA, Goddard Space Flight Center Greenbelt, Maryland 20771	1
Mr. James F. Connors, Chief Office of Research Plans and Programs NASA, Lewis Research Center 21000 Brookpark Road Cleveland, Ohio 44135	1
Mr. James E. Calkins Office of Research and Advanced Development NASA, Jet Propulsion Laboratory 4800 Oak Grove Drive Pasadena, California 91103	1
Mr. A. R. Raffaelli PR-2 NASA, John F. Kennedy Space Center Kennedy Space Center, Florida 32899	1
NASA/MTF Technical Library Bldg. 1100, Room C-111 Bay St. Louis, Mississippi 39520	1

CENTERS (Cont'd)

Dr. A. H. Knothe Code TEC NASA, John F. Kennedy Space Center Kennedy Space Center, Florida 32899	1
Mr. Robert Hinckley NASA, Electronics Research Center Room 323 B Cambridge, Massachusetts 02139	1
Dr. William G. Melbourne Mail Stop 180-300 Jet Propulsion Laboratory 4800 Oak Grove Drive Pasadena, California 91103	1
Scientific and Technical Information Facility Attn: NASA Rep. (S-AK/ RKT) P. O. Box 33 College Park, Maryland 20740	25
Mr. P. M. Caldwell Building 1105, Room 1105 National Aeronautics and Space Administration Mississippi Test Facility Bay St. Louis, Mississippi 39520	1

DEPARTMENT OF DEFENSE

Dr. William W. Carter Chief Scientist U. S. Army Missile Command Bldg. 5250 Redstone Arsenal, Alabama 35809	1
Mr. John McDaniel Technical Director Research and Development Directorate U. S. Army Missile Command Building 4505 Redstone Arsenal, Alabama 35809	12
Lt. Fred Alles Arnold Air Force Base Tullahoma, Tennessee 37389	30

CONTRACTORS

The Boeing Company Attn: Mr. John Pehrson P. O. Box 1680 Huntsville, Alabama 35807	5

CONTRACTORS

Brown Engineering Company, Inc. Mail Stop 5 300 Sparkman Drive, NW Huntsville, Alabama 35807	5
Chrysler Corporation Attn: Mr. Howard Blood 1312 Meridian, North Huntsville, Alabama 35804	5
Douglas Aircraft Holiday Office Center Huntsville, Alabama 35801	5
General Electric Company Suite 93 Holiday Office Center Huntsville, Alabama 35801	1
Hayes International Corporation 204 Oakwood Avenue, NE Huntsville, Alabama 35811	5
IBM Corporation 150 Sparkman Drive, NW Huntsville, Alabama 35807	5
Lockheed Aircraft Corporation Holiday Office Center Huntsville, Alabama 35801	5
North American Aviation, Inc. Holiday Office Center Huntsville, Alabama 35801	5
Northrop Corporation Holiday Office Center Huntsville, Alabama 35801	5
Mr. W. G. Calder General Electric Company Suite 13 Holiday Office Center Huntsville, Alabama 35801	1
The Boeing Company Attn: Mr. John Pehrson P. O. Box 1680 Huntsville, Alabama 35807	5
Library General Dynamics Fort Worth Division Fort Worth, Texas 76101	

CONTRACTORS (Cont'd)

Sperry Rand Corporation 8110 Memorial Parkway, SW Huntsville, Alabama 35802	5
Space Craft, Incorporated 8620 Memorial Parkway, SW Huntsville, Alabama 35802	1
Spaco, Incorporated 3022 University Drive, NW Huntsville, Alabama 35805	5
University of Alabama 4701 University Avenue, NW Huntsville, Alabama 35804	5
Vitro Corporation of America Holiday Office Center Huntsville, Alabama 35801	5
Wyle Laboratories Highway 20, West Huntsville, Alabama 35806	5
Mr. Robert Hardesty General Electric Company Ordinance Department 100 Plastics Avenue Room 1040 Pittsfield, Massachusetts 01201	1

UNIVERSITIES AND COLLEGES

Alabama A&M College Huntsville, Alabama 35811	1
University of Alabama Tuscaloosa, Alabama 35401	1
Dr. Clyde Hull Cantrell, Director Ralph Brown Draughon Library Auburn University Auburn, Alabama 36830	4
University of California (UCLA) Los Angeles, California 90024	1
Carnegie Institute of Technology Pittsburgh, Pennsylvania 15213	1
Case Institute of Technology Cleveland, Ohio 44106	1
Clemson University Clemson, South Carolina 29631 Attn: Mr. J. W. Gourlay	1

UNIVERSITIES AND COLLEGES (Cont'd)

Mr. S. G. Nicholas Director of Engineering Research Clemson University Clemson, South Carolina 29631	1
Columbia University New York, New York 10027	1
Librarian Columbia University Nevis Laboratories Irvington, New York 10533	1
University of Denver Denver, Colorado 80210	1
Director's Office Denver Research Institute University of Denver 80210 Denver, Colorado	1
Department of Nuclear Engineering Sciences University of Florida Gainesville, Florida 32603	1
Mrs J. Henley Crosland Director, Libraries Georgia Institute of Technology Atlanta, Georgia 30332	9
University of Georgia Athens, Georgia 30601	1
Louisiana State University Baton Rouge, Louisiana 70803	1
Massachusetts Institute of Technology Cambridge, Massachusetts 02138	1
University of Michigan Ann Arbor, Michigan 48106	1
Mississippi State University State College, Mississippi 39762	1
University of Mississippi University, Mississippi 38677	1
University of North Carolina Chapel Hill, North Carolina 27514	1

UNIVERSITIES AND COLLEGES (Cont'd)

Northeast Louisiana College Monroe, Louisiana 71201	1
Ohio State University Columbus, Ohio 43210	1
Ohio University Athens, Ohio 45701	1
Oklahoma State University Stillwater, Oklahoma 74074	1
University of Pittsburgh Pittsburgh, Pennsylvania 15213	1
Princeton University Princeton, New Jersey 08540	1
Library School of Electrical Engineering Purdue University Lafayette, Indiana 47907	1
Rev. R. J. Henle, S. J. Vice President for Academic Matters and Research Director Saint Louis University 221 N. Grand Blvd. St. Louis, Missouri 63103	2
Stanford University Palo Alto, California 94305	1
Syracuse University Syracuse, New York 13210	1
University of Tennessee Knoxville, Tennessee 37916	1
Cushing Memorial Library Texas A& M University College Station, Texas 77843	1
Mr. Harry E. Whitmore, Head Space Technology Division Texas A& M University College Station, Texas 77843	2
University of Texas Austin, Texas 78712	1

UNIVERSITIES AND COLLEGES (Cont'd)

Science Librarian Tulane University Library New Orleans, Louisiana 70118	1
The Joint University Libraries 419-21st Avenue, South Nashville, Tennessee 37203	1
Science Library Vanderbilt University Box 1521, Station B Nashville, Tennessee 37203	1
Virginia Polytechnic Institute Blacksburg, Virginia 24061	1
Washington State Pullman, Washington 99163	1
Mr. H. W. Hsu Associate Professor of Chemical Engineering University of Tennessee Knoxville, Tennessee 37916	1
Professor F. N. Peebles Department of Engineering Mechanics University of Tennessee Knoxville, Tennessee 37916	1
Mr. W. Byron Long Director of Special Projects Mississippi Research and Development Center Jackson, Mississippi 39205	1
Engineering Library University of Arkansas Fayetteville, Arkansas 72701	1
Mr. Carl O. Thomas Associate Dean, Graduate School University of Tennessee Knoxville, Tennessee 37916	1

UNITS OF MEASURE

In a prepared statement presented on August 5, 1965, to the U. S. House of Representatives Science and Astronautics Committee (chaired by George P. Miller of California), the position of the National Aeronautics and Space Administration on Units of Measure was stated by Dr. Alfred J. Eggers, Deputy Associate Administrator, Office of Advanced Research and Technology:

"In January of this year NASA directed that the international system of units should be considered the preferred system of units, and should be employed by the research centers as the primary system in all reports and publications of a technical nature, except where such use would reduce the usefulness of the report to the primary recipients. During the conversion period the use of customary units in parentheses following the SI units is permissible, but the parenthetical usage of conventional units will be discontinued as soon as it is judged that the normal users of the reports would not be particularly inconvenienced by the exclusive use of SI units."

The International System of Units (SI Units) has been adopted by the U. S. National Bureau of Standards (see NBS Technical News Bulletin, Vol. 48, No. 4, April 1964).

The International System of Units is defined in NASA SP-7012, "The International System of Units, Physical Constants, and Conversion Factors," which is available from the U. S. Government Printing Office, Washington, D. C. 20402.

SI Units are used preferentially in this series of research reports in accordance with NASA policy and following the practice of the National Bureau of Standards.